

# PROLITH: a comprehensive optical lithography model

Chris A. Mack

Department of Defense  
Fort Meade, MD 20755-6000

## ABSTRACT

The Positive Resist Optical Lithography model (PROLITH) is introduced. The model predicts resist profiles for submicron projection, proximity and contact printing. Included are models for optical projection systems, the standing wave effect for projection printing, a diffraction model for contact printing, a kinetic model for the exposure reaction, and a kinetic model of the development process. Also included in PROLITH are the effects of prebake conditions and polychromatic exposure.

## INTRODUCTION

Process modeling has become an increasingly important tool in semiconductor research and manufacturing. One of the most important uses of process modeling is to optimize the performance of a process for smaller and smaller dimensions. The eventual production of submicron geometry devices requires that one process step in particular be pushed to its physical limits: optical lithography. If a model is to be useful in predicting the performance of a lithography system, it must be capable of modeling in the submicron regime.

Past lithography modeling efforts have centered around the work of Dill, et al,<sup>(1)</sup> which models projection exposure and development of positive resists. Other models<sup>(2)</sup> have added features and made slight changes, but are still limited to projection lithography. The need for a model for contact printing has been expressed by researchers<sup>(3)</sup> and could become a limited production need. In this paper the Positive Resist Optical Lithography model (PROLITH) is introduced. The model applies not only to projection printing but to proximity and contact printing as well. It incorporates the effects of prebake conditions on exposure and development and allows for polychromatic exposure. PROLITH is designed to be a versatile, comprehensive submicron optical lithography model.

## PROJECTION PRINTING

Of the three major types of optical lithography in use today (projection, proximity and contact printing), projection printing is the easiest to model<sup>(1,2)</sup>. This is due to the fact that the intensity of the exposing radiation within the resist  $I(x,y,z)$  is separable, ie,

$$I(x,y,z) = I_i(x,y)I_s(z) \quad (1)$$

where  $I_i(x,y)$  = the projected image intensity on the surface of the resist film

$I_s(z)$  = relative intensity due to the standing wave effect.

$I_i(x,y)$  is dependent only on the projection printer and is independent of the resist.  $I_s(z)$  is dependent only on the resist system and independent of the projection printer (with the exception of wavelength). Thus, the two may be calculated independently.

Determining  $I_i(x,y)$  requires an analysis of the optical system used to produce the image. The parameters of importance are the wavelength of the exposing radiation,  $\lambda$ , the numerical aperture of the objective lens,  $NA_0$ , the shape of the aperture, the degree of coherence,  $\sigma$ , the deviation (if any) of the resist surface from the plane of perfect focus (called the defocus distance),  $\delta$ , and of course the geometry of the feature to be imaged. The theoretical principles required to model such a system was first given by Hopkins<sup>(4-6)</sup> and have been applied to the problem of projection printing<sup>(7-9)</sup>. The results of such an analysis can be seen in Figure 1.

When a thin photoresist film on a reflecting substrate is exposed to monochromatic light, standing waves are produced in the resist. The effects of standing waves on linewidth control and resolution have been well documented<sup>(10-14)</sup>. Several methods of calculating the standing wave intensity  $I_s(z)$  have been proposed,<sup>(13,14)</sup> but all have been in the form of numerical approximations. It can be shown that a closed form solution for  $I_s(z)$  exists for the case of projection printing. Consider a homogeneous thin photoresist film of thickness  $D$  and complex index of refraction  $n_2$  deposited on a thick substrate with complex index of refraction  $n_3$  in an ambient environment of index  $n_1$ . Let  $E_2(x,y,z)$  be the electric field in the photoresist (see Figure 2). If the film is illuminated by a normally incident plane wave  $E_1(x,y)$ , the electric field within the resist is given by

$$E_2(x,y,z) = E_1(x,y)v_{12} \frac{\exp(-ik_z z) + \rho_{23}v_D^2 \exp(ik_z z)}{1 + \rho_{12}\rho_{23}v_D^2} \quad (2)$$

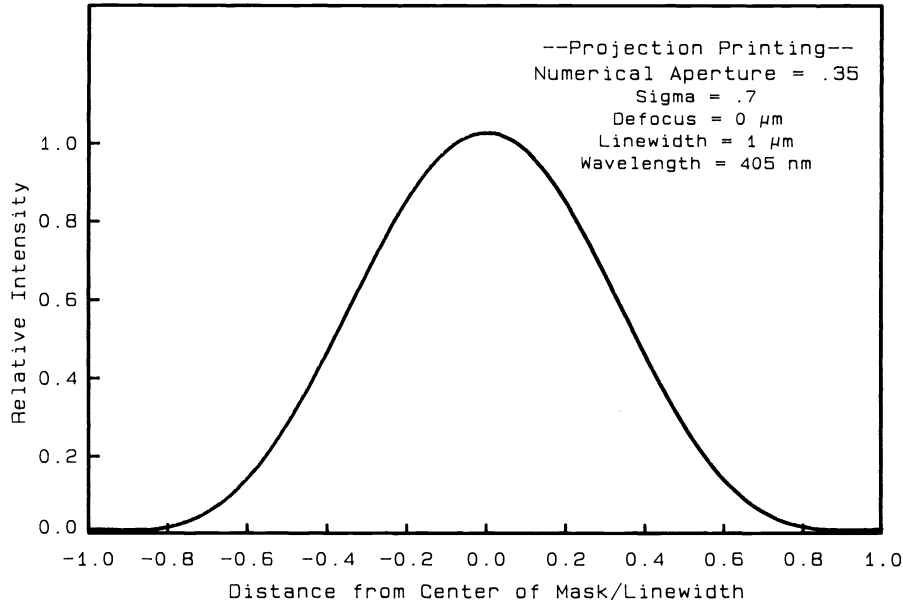


Figure 1 : Image intensity for a partially coherent projection printer.

- where  $\rho_{ij} = (n_i - n_j)/(n_i + n_j)$ , the reflection coefficient  
 $\tau_{ij} = 2n_i/(n_i + n_j)$ , the transmission coefficient  
 $\tau_D = \exp(-ik_2D)$ , the internal transmittance of the resist  
 $k_j = 2\pi n_j/\lambda$ , the propagation constant of media  $j$   
 $n_j = n_j - iK_j$ , the complex index of refraction of media  $j$ .

For a weakly absorbing film, the imaginary parts of  $\rho_{12}$  and  $\tau_{12}$  can be neglected and the intensity can be calculated from

$$I_S(z) = I_0 \tau_{12}^2 e^{-\alpha z} \frac{1 + g(D-z) + |\rho_{23}|^2 e^{-\alpha 2(D-z)}}{1 + \rho_{12}^2 g(D) + \rho_{12}^2 |\rho_{23}|^2 e^{-\alpha 2D}} \quad (3)$$

where  $g(\Delta) = 2e^{-\alpha \Delta} [\text{re}\{\rho_{23}\} \cos(4\pi n_2 \Delta/\lambda) + \text{im}\{\rho_{23}\} \sin(4\pi n_2 \Delta/\lambda)]$   
 $\alpha = 4\pi k_2/\lambda$ , the absorption coefficient of medium 2.

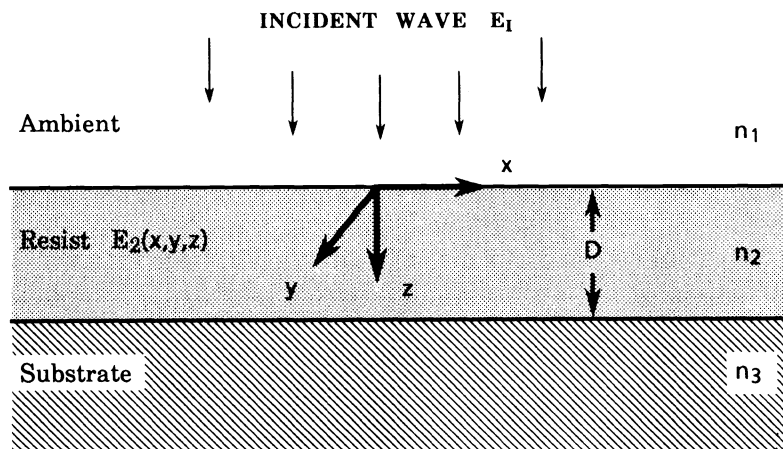


Figure 2 : Geometry used in the derivation of the standing wave intensity.

As can be seen from equation (3), the intensity within the thin film varies sinusoidally with a period of  $\lambda/2n_2$ . There will be a minimum intensity at the film-substrate interface ( $z=D$ ) for a reflecting substrate ( $\rho_{23}$  negative). This minimum will be zero for a perfectly reflecting substrate ( $\rho_{23} = -1$ ). The factor  $e^{-az}$  accounts for absorption by the film, where  $az$  is called the absorbance  $A$ .

It is very common to have more than one film coated on a substrate. The problem then becomes that of two or more absorbing thin films on a substrate. An analysis similar to that shown above for one film yields the following result for the electric field in the top film of an  $m-1$  layer system:

$$E_2(x,y,z) = E_1(x,y) \tau_{12} \frac{\exp(-ik_2z) + \rho'_{23} \tau_{D2}^2 \exp(ik_2z)}{1 + \rho_{12} \rho'_{23} \tau_{D2}^2} \quad (4)$$

where

$$\rho'_{23} = \frac{n_2 - n_3 X_3}{n_2 + n_3 X_3}$$

$$X_3 = \frac{1 - \rho'_{34} \tau_{D3}^2}{1 + \rho'_{34} \tau_{D3}^2}$$

$$\rho'_{34} = \frac{n_3 - n_4 X_4}{n_3 + n_4 X_4}$$

$$\vdots$$

$$\vdots$$

$$\vdots$$

$$X_m = \frac{1 - \rho_{m,m+1} \tau_{Dm}^2}{1 + \rho_{m,m+1} \tau_{Dm}^2}$$

$$\rho_{m,m+1} = \frac{n_m - n_{m+1}}{n_m + n_{m+1}}$$

$$\tau_{Dj} = \exp(-ik_j D_j)$$

and all other parameters are defined previously. The parameter  $\rho'_{23}$  is the effective reflection coefficient between the thin film and what lies beneath it. A graph of equation (4) is shown in Figure 3. If the thin film in question is not the top film (layer 2), the intensity can be calculated in layer  $j$  from

$$E_j(x,y,z) = E_{I(eff)} \tau_{j-1,j}^* \frac{\exp(-ik_j z_j) + \rho'_{j,j+1} \tau_{Dj}^2 \exp(ik_j z_j)}{1 + \rho_{j-1,j}^* \rho'_{j,j+1} \tau_{Dj}^2} \quad (5)$$

where  $\tau_{j-1,j}^* = 1 + \rho_{j-1,j}^*$  and

$$\rho_{j-1,j}^* = \frac{n_{j-1} Y_{j-1} - n_j}{n_{j-1} Y_{j-1} + n_j}$$

$$Y_{j-1} = \frac{1 + \rho_{j-2,j-1}^* \tau_{Dj-1}^2}{1 - \rho_{j-2,j-1}^* \tau_{Dj-1}^2}$$

$$\rho_{23}^* = \frac{n_2 Y_2 - n_3}{n_2 Y_2 + n_3}$$

$$Y_2 = \frac{1 + \rho_{12} \tau_{D2}^2}{1 - \rho_{12} \tau_{D2}^2}$$

$$\rho_{12} = \frac{n_1 - n_2}{n_1 + n_2}$$

$$E_{I(\text{eff})} = E_I \frac{\tau_{12} \tau_{D2}}{1 + \rho_{12} \tau_{D2}^2} \frac{\tau_{23}^* \tau_{D3}}{1 + \rho_{23}^* \tau_{D3}^2} \dots \frac{\tau_{j-2j-1} \tau_{Dj-1}}{1 + \rho_{j-2j-1}^* \tau_{Dj-1}^2}$$

and  $z_j$  is the distance into layer  $j$ . The effective reflection coefficient  $\rho^*$  is analogous to the coefficient  $\rho'$ , looking in the opposite direction.

If the film in question is not homogeneous the equations above are, in general, not valid. Let us, however, examine one special case in which the inhomogeneity takes the form of variations in the imaginary part of the index of refraction of the film, leaving the real part constant. In this case, the absorbance  $A$  is no longer simply  $az$ , as in the homogeneous case, but becomes

$$A(z) = \int_0^z a(z') dz' \quad (6)$$

It can be shown that equation (3) is still valid if the anisotropic expression for absorbance (6) is used.

$$I_s(z) = I_0 \tau_{12}^2 e^{-A(z)} \frac{1 + g(D-z) + |\rho_{23}|^2 e^{-2A(D-z)}}{1 + \rho_{12}^2 g(D) + \rho_{12}^2 |\rho_{23}|^2 e^{-2A(D)}} \quad (7)$$

where  $g(\Delta) = 2e^{-A(\Delta)}[\text{re}\{\rho_{23}\}\cos(4\pi n_2 \Delta/\lambda) + \text{im}\{\rho_{23}\}\sin(4\pi n_2 \Delta/\lambda)]$ . Thus,  $I_s(z)$  can be found if the absorption coefficient is known as a function of  $z$ . For an AZ-type positive photoresist, the absorption coefficient is related to the concentration of light sensitive material within the resist<sup>(15)</sup>.

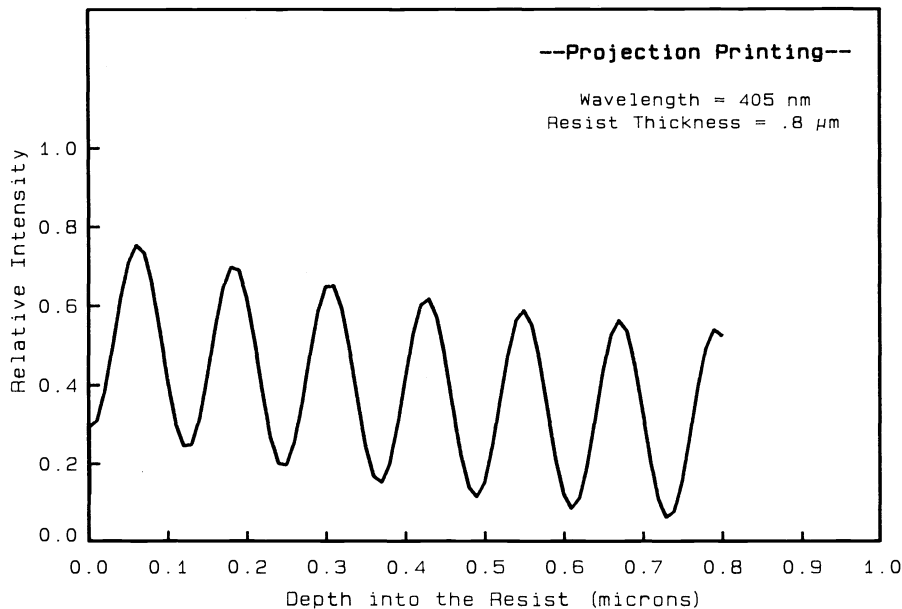


Figure 3 : Standing wave intensity for Kodak 820 resist on 60nm oxide over silicon.

$$a(z) = A m(z) + B \quad (8)$$

where A, B are measurable constants and m(z) is the relative concentration of photoactive compound (PAC). Determining m(z) is discussed in the section Photoresist Exposure Kinetics.

## CONTACT PRINTING

Unfortunately, the intensity within the resist I(x,y,z) is not separable for the cases of proximity and contact printing. These lithographies use a mask located some distance z<sub>gap</sub> above the resist surface. The problem is then one of calculating the diffraction pattern emanating from the mask feature and determining how this pattern is affected by the resist-substrate configuration.

The phenomenon of diffraction has been extensively studied and is well documented in the literature (e.g., reference 16). However, rigorous treatments of the problem are prohibitively complicated and thus, practical solutions make one or more simplifying approximations or assumptions. The most common practical treatment of diffraction is that given by Kirchoff. As with any approximate solution, Kirchoff's diffraction theory is appropriate only under certain conditions, and this region of validity is outlined below. Of course, any theory is useful only if it can be applied to realistic situations. Thus, a method for applying Kirchoff's theory to heterogeneous media (in particular those media appropriate to contact printing) will be given.

Consider an electromagnetic wave U<sub>I</sub> incident on a black screen with an aperture A. The electric field at some point P on the other side of the screen is given by Kirchoff's diffraction integral.

$$U(P) = \frac{1}{4\pi} \int \int_A (U_I \partial G / \partial n - G \partial U_I / \partial n) dS \quad (9)$$

where n is the direction normal to the aperture and G is Green's function which is defined for a homogeneous media by

$$G = \frac{e^{iks}}{s} \quad (10)$$

where s is the distance from the point P to the point (x,y,z) on the aperture A. In general, Green's function can be thought of as the response of the media to a point source located at P. Thus, if U<sub>I</sub> is known at the aperture, U(P) can be determined. As a specific example, consider a plane wave E<sub>I</sub> traveling in the z-direction which is diffracted by an infinite slit of width w in the x-y plane. Equation (9) becomes

$$U(P) = C \frac{E_I}{4\pi} \int_{-\frac{w}{2}}^{\frac{w}{2}} \left[ \frac{\partial G(x_s, P)}{\partial z} + ik_1 G(x_s, P) \right] dx_s \quad (11)$$

$$\text{where } C = \left[ \frac{z\lambda}{2} \right]^{1/2} (1+i).$$

Kirchoff's integral applies to diffraction in a homogeneous media. For the case of contact printing, the media consists of several layers of different material (Figure 2). If these layers are assumed to be homogeneous within each layer, and are all parallel to the plane of the mask (ie, in the x-y plane), one can show that the electric field in the second layer (the photoresist) can be calculated from

$$\begin{aligned} U_x(P) &= \frac{1}{4\pi} \int \int_A (U_{Ix} \partial G / \partial n - G \partial U_{Ix} / \partial n) dS \\ U_y(P) &= \frac{1}{4\pi} \int \int_A (U_{Iy} \partial G / \partial n - G \partial U_{Iy} / \partial n) dS \\ U_z(P) &= \frac{n_1^2}{4\pi n_2} \int \int_A (U_{Iz} \partial G / \partial n - G \partial U_{Iz} / \partial n) dS \end{aligned} \quad (12)$$

where the Green's function has several important restrictions. In layer 2 (the photoresist), Green's function takes the form

$$G = \exp(ik_2 s) / s + g(P, Q) \quad (13)$$

where  $Q$  = a point on the aperture  $A$

$s$  = distance from  $P$  to  $Q$

$$k_2 = 2\pi n_2 / \lambda .$$

The function  $g(P,Q)$  must be a solution of the wave equation and have continuous first and second derivatives within and at the boundaries of layer 2. Further,  $G$  and  $\partial G / \partial z$  must be continuous in each layer and be continuous across the boundary of each layer.

As an example of the use of these equations, consider that given above for a plane wave normally incident on an infinitely long slit.  $U_1$ , the incident wave, has no  $z$  component, thus the last of the three equations (12) is zero. The first two equations become

$$U_x(P) = C \frac{U_{Ix}}{4\pi} \int_{-\frac{w}{2}}^{\frac{w}{2}} \left[ \frac{\partial G(x_s, P)}{\partial z} + ik_1 G(x_s, P) \right] dx_s$$

$$U_y(P) = C \frac{U_{Iy}}{4\pi} \int_{-\frac{w}{2}}^{\frac{w}{2}} \left[ \frac{\partial G(x_s, P)}{\partial z} + ik_1 G(x_s, P) \right] dx_s \tag{14}$$

and the intensity at  $P$  becomes

$$I(P) = I_I \left[ C \frac{1}{4\pi} \int_{-\frac{w}{2}}^{\frac{w}{2}} \left[ \frac{\partial G(x_s, P)}{\partial z} + ik_1 G(x_s, P) \right] dx_s \right]^2 . \tag{15}$$

It is interesting to note that the above expression for intensity is identical to the expression one would obtain for the case of a homogeneous media (i.e., from equation (11)), the only difference being the choice of the Green's function.

In the above discussion we have placed many restrictions on  $G$  and the usefulness of equation (15) will depend on our ability to determine a suitable function for  $G$ . The Green's function must satisfy the homogeneous wave equation in each layer, it must be continuous and have a continuous first derivative across each boundary, and it must take the form of equation (13) in layer 2. As was mentioned previously, the Green's function can be thought of as the response of the system to a point source at  $P$ . It can be shown that this response meets the three conditions above. We shall now determine the Green's function for a specific case.

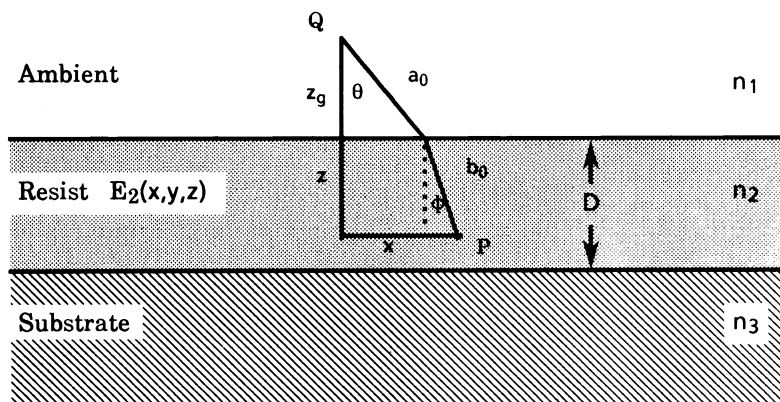


Figure 4 : Geometry used in determining Green's function.

Consider a medium which consists of air over resist over a reflecting substrate (Figure 4). The electric field distribution within the aperture  $A$  due to a point source at the point  $P$  within the resist must be determined. An

equivalent though conceptually simpler problem is determining the electric field at P due to a point source Q within the aperture. Consider the geometry shown in Figure 4. For simplicity, the coordinate system has been defined so that  $z=0$  on the resist surface. A geometrical approach will be used in which the electric field at an arbitrary point in the resist P is the sum of the rays emanating from the point source Q which pass through P. The first ray is simply refracted at the resist surface to pass through P(x,z). Using Snell's Law and the geometry of the situation:

$$\begin{aligned}
 a_o &= z_g / \cos\phi \\
 b_o &= z / \cos\theta \\
 \cos\phi &= \left(1 - \frac{n_2^2}{n_1^2} \sin^2\theta\right)^{1/2} \\
 \cos\theta &= (1 - \sin^2\theta)^{1/2}
 \end{aligned} \tag{16}$$

Determining the angle  $\theta$  is more complicated than it may seem. The function  $\theta(z, z_g, x)$  is transcendental and must be solved iteratively. The transmission and reflection coefficients must be defined for oblique incidence.

$$\begin{aligned}
 \tau_{12} &= \frac{2n_1 \cos\phi}{n_1 \cos\phi + n_2 \cos\theta} \\
 \rho_{21} &= \frac{n_2 \cos\theta - n_1 \cos\phi}{n_2 \cos\theta + n_1 \cos\phi} \\
 \rho_{23} &= \frac{n_2 \cos\theta - (n_3^2 - n_2^2 \sin^2\theta)^{1/2}}{n_2 \cos\theta + (n_3^2 - n_2^2 \sin^2\theta)^{1/2}}
 \end{aligned} \tag{17}$$

Since either parallel or perpendicular polarization will yield equivalent results, perpendicular polarization has been chosen. The electric field due to a ray with no reflections  $E_o$  becomes

$$E_o = \frac{\tau_{12}(\theta)}{a_o + b_o} \exp(-i[k_1 a_o + k_2 b_o]) \tag{18}$$

The next ray to be considered has one reflection (off the substrate). Let  $a_1$  be the distance the ray travels in air and  $b_1$  the distance the ray travels in the resist. It can be shown that equations (16) will give the proper results if the variable  $z$  is replaced by  $z_1$  where

$$z_1 = 2D - z \tag{19}$$

Similarly, after  $n$  reflections equations (16) are true when  $z$  is replaced by  $z_n$  where

$$z_n = \begin{cases} nD + z, & \text{for } n \text{ even} \\ (n+1)D - z, & \text{for } n \text{ odd.} \end{cases} \tag{20}$$

The expression for the electric field caused by a ray undergoing  $n$  reflections becomes, for  $n$  even:

$$E_n = \frac{\tau_{12}(\theta) [\rho_{23}(\theta) \rho_{21}(\theta)]^{n/2}}{a_n + b_n} \exp(-i[k_1 a_n + k_2 b_n])$$

for  $n$  odd:

$$E_n = \frac{r_{12}(\theta) \rho_{23}(\theta) [\rho_{23}(\theta) \rho_{21}(\theta)]^{(n-1)/2}}{a_n + b_n} \exp(-i[k_1 a_n + k_2 b_n]) \quad (21)$$

The total electric field at the point P(x,z) is then the sum of each ray.

$$G = \sum_{n=0}^{\infty} E_n \quad (22)$$

Fortunately, the series (22) converges very rapidly, within five or six terms using typical resist parameters.

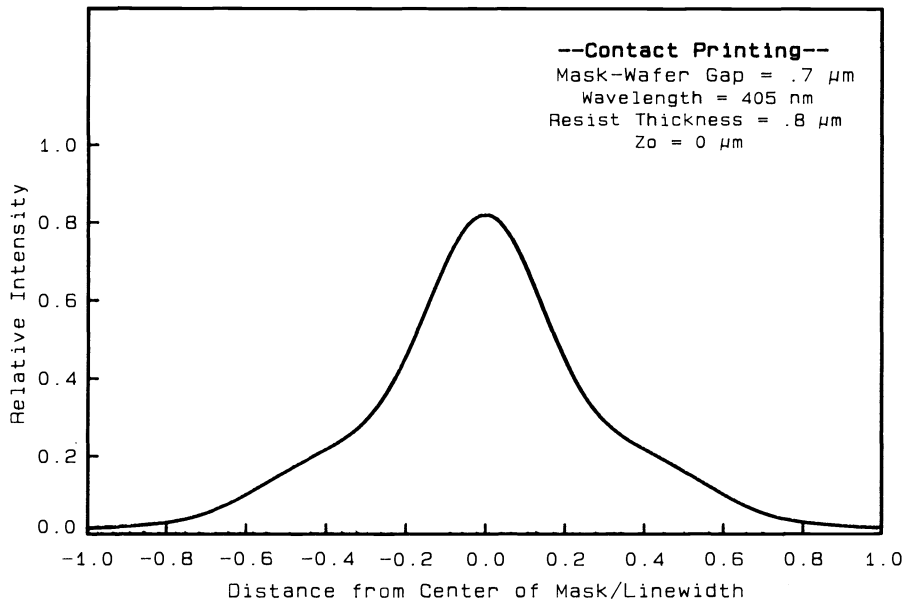


Figure 5 : Diffraction pattern within the resist for an infinite slit.

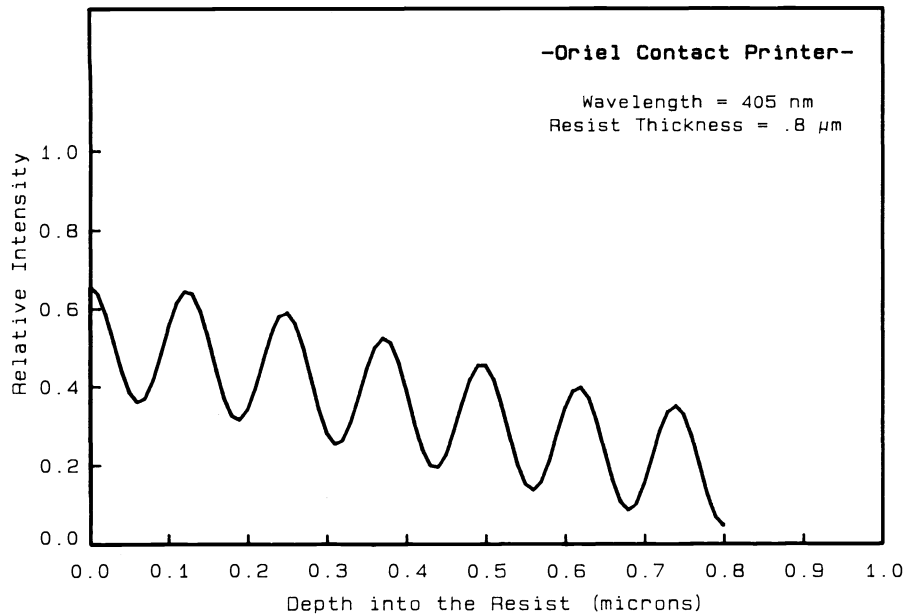


Figure 6 : "Standing Wave" pattern for contact printing.

Using the above formulation of Green's function, the intensity within the resist can be determined using equation (15). The results for a typical contact printing situation are shown in Figures 5 and 6. Kirchoff's integral has been found to be valid for values of  $z_{\text{gap}}$  greater than about a wavelength, making this type of solution inappropriate for conformable contact printing, where  $z_{\text{gap}}$  can be much less than a wavelength<sup>(17)</sup>. The problem then becomes one of solving Maxwell's equations for a given set of boundary conditions<sup>(18,19)</sup>.



## PHOTORESIST EXPOSURE KINETICS

The standard AZ-type positive photoresist is composed of three parts; a solvent S, a resin R, and a photoactive compound (PAC), also called an inhibitor, M. When exposed to UV radiation, the PAC reacts to form a product P.



The PAC inhibits the dissolution of the resist in developer (which is usually a basic aqueous solution), whereas the product enhances dissolution of the resist, thus giving the resist its image reproduction properties. An understanding of the kinetics of the exposure reaction (23) allows one to determine the amount of PAC that reacts for a given exposure time and intensity. The result of a kinetic analysis is

$$M = M_0 \exp(-ct) \quad (24)$$

where  $M_0$  = initial PAC concentration (i.e., before exposure)

$c$  = rate constant

$I$  = exposure intensity

$t$  = exposure time.

Although equation (24) applies to monochromatic radiation, it can be applied also to polychromatic exposure when  $c$  is replaced by  $c_{eff}$  as defined by

$$c_{eff} = \frac{\int c(\lambda) I_R(\lambda) d\lambda}{\int S_D(\lambda) I_R(\lambda) d\lambda} \quad (25)$$

where  $c(\lambda)$  = exposure constant at wavelength  $\lambda$

$S_D(\lambda)$  = spectral sensitivity of the detector used to measure the light

$I_R(\lambda)$  = relative intensity of the source at wavelength  $\lambda$

and the intensity  $I$  in equation (24) becomes the measured intensity.

As was discussed in the previous section, the intensity of the exposing light is a function of position within the resist. It is also a function of time due to the changing concentration of PAC during exposure. If the image in question is an infinitely long slit in the  $y$ -direction, the intensity is a function of  $x$ ,  $z$  and  $t$ . Equation (24) becomes

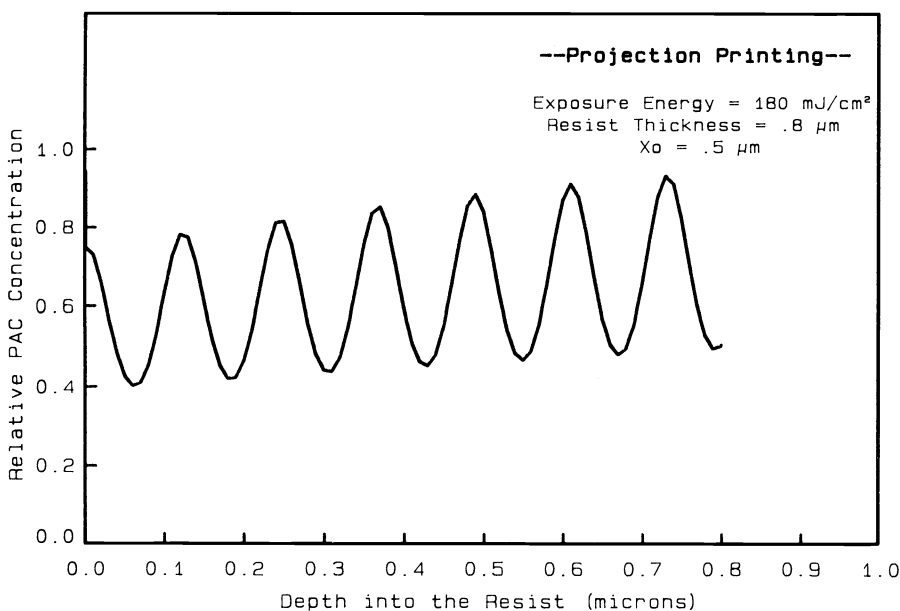


Figure 7 : Relative PAC concentration as a function of depth into the resist.

$$m(x,z,t) = \exp(-cI(x,z,t)t) \quad (26)$$

where the relative PAC concentration,  $m$ , is simply  $M/M_0$ . Using the analysis techniques described for standing waves, one can determine  $I(x,z,0)$ . If we divide the exposure time into a series of small time increments  $\Delta t$  so that  $t = \Sigma \Delta t$ , we can calculate the relative PAC concentration after an exposure of  $\Delta t$  duration. Knowing  $m(x,z)$  at time  $\Delta t$ , we can recalculate  $I(x,z,\Delta t)$  using equation (7). This can then be used to calculate  $m(x,z,2\Delta t)$ , and so on until the time  $t$  is reached. A plot of  $m(0,z,t)$  for a typical exposure is shown in Figure 7.

## DEVELOPMENT MECHANISM

Once  $m(x,z)$  is known for the exposed photoresist, a development model can be used to predict what parts of the resist will be dissolved by the developer. For this purpose, one must know the rate of dissolution of the resist as a function of the relative PAC concentration  $m(x,z)$ . Previous attempts at defining a development rate equation have been empirical "curve-fits" of experimental data<sup>(15)</sup> and pseudo-empirical fits where an assumed form is given to the development rate curve and appropriate constants are determined from the experimental data<sup>(20)</sup>. The assumed shape, however, has no physical basis and, therefore, is still empirical in nature. A more appropriate development rate model should be based on the chemical process of development and should be derived from a kinetic analysis of this process.

The development of a resist involves three processes: diffusion of developer from the bulk solution to the surface of the resist, reaction of the developer with the resist, and diffusion of the product back into the solution. For this analysis we shall assume that the last step, diffusion of the dissolved resist into solution, occurs very quickly so that this step may be ignored. Let us now look at the first two steps in the proposed mechanism. The diffusion of developer to the resist surface can be described with the simple diffusion rate equation:

$$r_D = -k_D(D - D_s) \quad (27)$$

where  $r_D$  = rate of diffusion of the developer to the resist surface

$D$  = bulk developer concentration

$D_s$  = developer concentration at the resist surface

$k_D$  = rate constant.

We shall now propose a mechanism for the reaction of developer with the resist. The resin is somewhat soluble in the developer solution, but the presence of the PAC acts as an inhibitor to dissolution, making the development rate very slow. The product  $P$ , however, is very soluble in developer. The presence of  $P$  enhances the dissolution rate of the resin. Let us assume that  $n$  molecules of product  $P$  must be present in order to dissolve a resin molecule. The rate of the reaction is

$$r_R = -k_R D_s P^n \quad (28)$$

where  $r_R$  = the rate of reaction of the developer with the resist

$k_R$  = rate constant.

From the stoichiometry of the exposure reaction

$$P = M_0 - M \quad (29)$$

The two steps outlined above are in series, i.e., one reaction follows the other. Thus, the two steps will come to a steady state such that

$$r_R = r_D = r \quad (30)$$

Equating the two rate equations, one can derive an expression for the development rate  $r$ ,

$$r = r_{max} \frac{(a+1)(1-m)^n}{a + (1-m)^n} + r_{min} \quad (31)$$

where  $r$  = development rate (nm/sec)

$r_{max}$  = development rate of fully exposed resist

$$r_{max} = \frac{k_D D}{k_D/k_R M_o^n + 1}$$

$r_{min}$  = development rate of unexposed resist

$n$  = developer selectivity (an experimentally determined constant)

$$a = k_D/k_R M_o^n$$

$$a = \frac{(n+1)}{(n-1)} (1 - m_{TH})^n$$

$m_{TH}$  = the threshold relative PAC concentration.

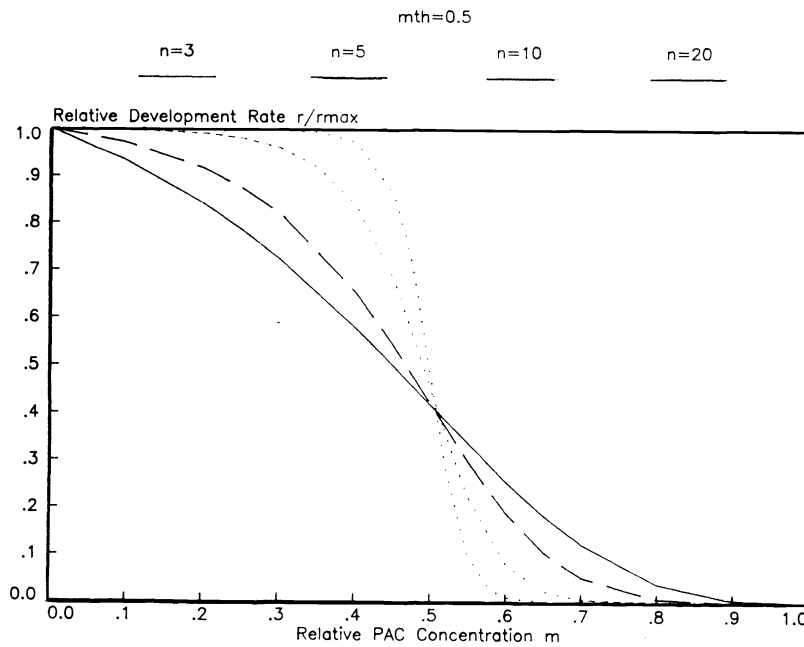


Figure 8 : Theoretical development rate curves using equation (31).

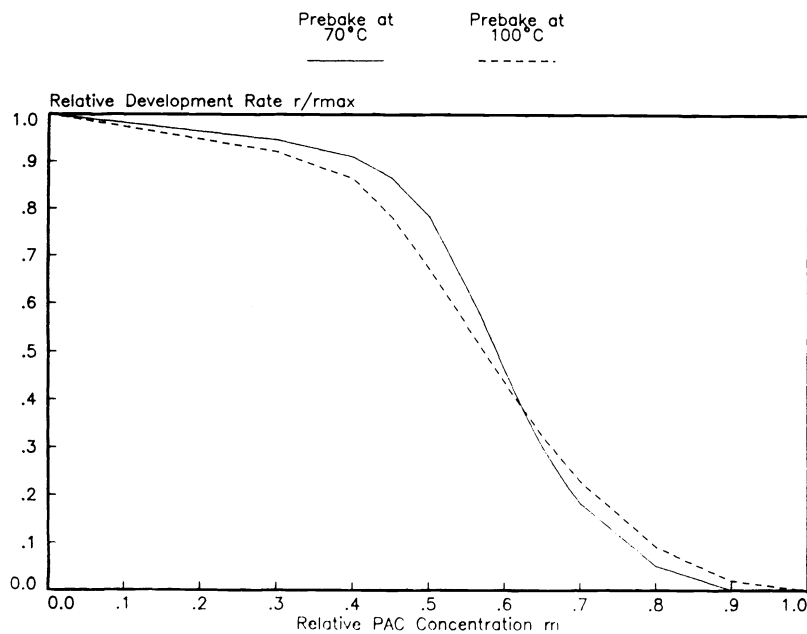


Figure 9 : Experimental development rate data (from Dill, et al. (15)).

The threshold concentration is defined as the value of  $m$  at which the development rate curve exhibits a point of inflection, ie,

$$\left. \frac{d^2r}{dm^2} \right|_{m_{TH}} = 0 .$$

The rate constants  $r_{max}$ ,  $r_{min}$ ,  $n$ , and  $m_{TH}$  must be determined in order to define the rate of dissolution of resist in the developer. From a resist processing point of view  $n$  can be thought of as a selectivity of the developer towards the exposed resist (Figure 8). Higher values of  $n$  result in higher selectivity. Of course,  $m_{TH}$  describes the threshold effect of development. Values of  $m < m_{TH}$  result in very high development rates, whereas values of  $m > m_{TH}$  give very low development rates. Also, one should note that  $r_{max}$  is proportional to the developer concentration  $D$ , but  $m_{TH}$  and  $n$  are independent of  $D$ . All parameters, however, are dependent on the resist and developer used. Experimental data collected by Dill, et al,<sup>(15)</sup> for AZ1350 resist with 1:1 AZ developer (Figure 9) is described very well by (31) with the constants given in Table I.

The reaction mechanism model proposed above addresses many of the problems associated with earlier empirical models. Physically, the model gives insight into the development process on microscopic and macroscopic levels. The threshold behavior of resist development is well known, but can now be quantified by  $m_{TH}$ . This parameter, along with the selectivity term  $n$ , can be used to compare the performance of different resist-developer systems in a meaningful way. For example, the use of a 70°C prebake was shown in Table I to give a higher selectivity than a 100°C prebake, making the latter temperature less desirable. Also, empirical models can not, in general, be used to describe other development processes in which experimental conditions have changed. Variations in developer concentration, for example, do not require the use of a new set of parameters, only a different value of  $r_{max}$ . Variations in prebake conditions can also be modeled as a change in  $M_0$  and new values of  $r_{max}$  and  $n$  can be determined. The temperature dependence of the various parameters can also be predicted using the standard Arrhenius plots to determine activation energies.

TABLE I

Development Parameters for AZ1350J in 1:1 AZ developer, based on the experimental data of Dill, et. al.<sup>(15)</sup>.

Prebake at 70°C 1 hour	Prebake at 100°C 1 hour
$r_{max} = 55 \text{ nm/s}$	$r_{max} = 21 \text{ nm/s}$
$n = 6$	$n = 5$
$m_{TH} = 0.61$	$m_{TH} = 0.61$
$r_{min} = 0.15 \text{ nm/s}$	$r_{min} = 2 \text{ nm/s}$

## DISCUSSION AND RESULTS

Using the principles and techniques described above one can model the processes of projection, proximity and contact printing. The result of such a model is a predicted resist profile. Two predicted profiles are given in Figures 10 and 11 for projection and contact printing, respectively.

PROLITH is a fortran language computer model incorporating the principles outlined above. It contains, however, several other features not discussed above. The prebake process can be modeled as a decomposition of photoactive compound to a non-photoreactive compound. The result is a decrease in the value of  $M_0$  in equation (24). The resist parameters  $A$  and  $B$  in equation (8) are also dependent on the initial PAC concentration, and thus on the prebake conditions. Development rates are effected by prebake in the form of the surface induction effect (a reduced development rate at the surface of the resist). All of these effects are taken into account by PROLITH. Post-exposure bakes are modeled as the diffusion of PAC within the resist.

PROLITH is designed for both user ease and flexibility. The current version runs on an IBM PC and makes full use of the PC's graphics capabilities to provide meaningful data output. Copies are available upon request.

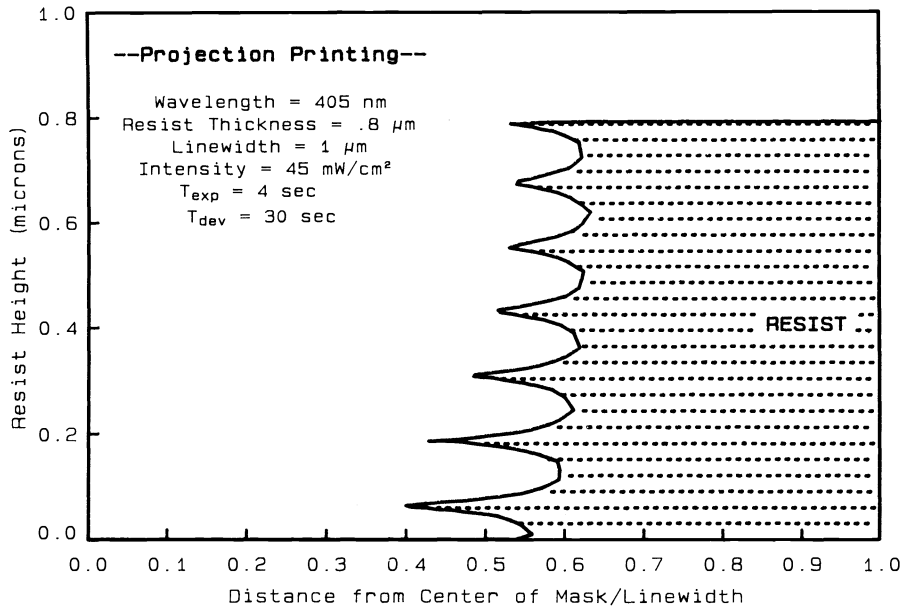


Figure 10 : Predicted resist profile for projection printing.

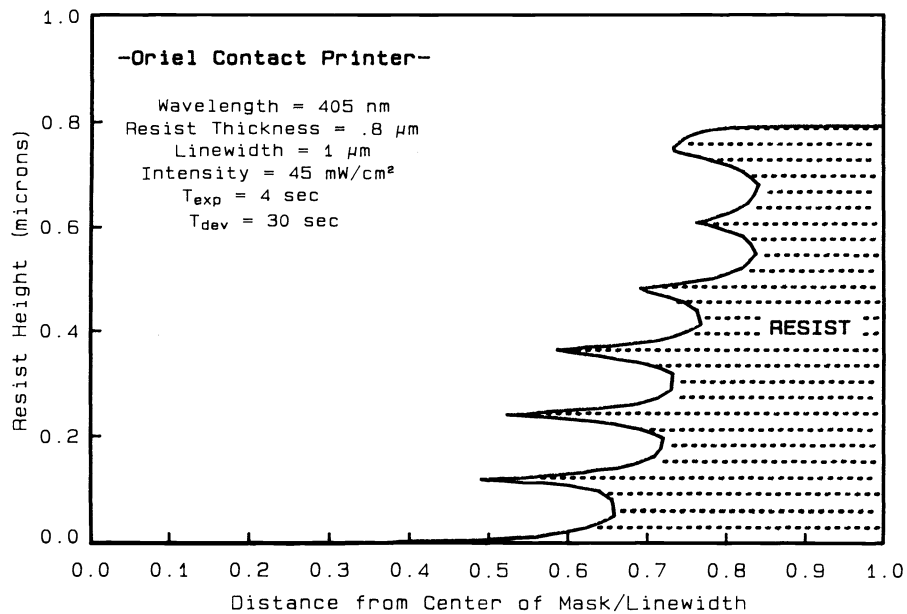


Figure 11 : Predicted resist profile for contact printing.

## REFERENCES

1. F. H. Dill, et al, "Modeling Projection Printing of Positive Photoresists," *Trans. Electron Dev.*, Vol. ED-22, No. 7, (July, 1975) pp. 456-464.
2. W. G. Oldham, et al, "A General Simulator for VLSI Lithography and Etching Processes: Part I - Application to Projection Lithography," *Trans. Electron Dev.*, Vol. ED-26, No. 4, (April, 1979) pp. 717-722.
3. H. I. Smith, N. Efremow and P. L. Kelly, "Photolithographic Contact Printing of 4000 Å Linewidth Patterns," *Jour. Electrochem. Soc.*, Vol. 121, No. 11, (November, 1974) pp. 1503-1506.
4. H. H. Hopkins, "The Concept of Partial Coherence in Optics," *Proc. Royal Soc. London*, Vol. A208, (1951) pp. 263-277.
5. H. H. Hopkins, "On the Diffraction Theory of Optical Images," *Proc. Royal Soc. London*, Vol. A217, (1953) pp. 408-432.
6. H. H. Hopkins, "The Frequency Response of a Defocused Optical System," *Proc. Royal Soc. London*, Vol. A231, (1955) pp. 91-103.
7. E. C. Kintner, "Method for the Calculation of Partially Coherent Imagery," *Appl. Optics*, Vol. 17, No. 17, (Sep. 1, 1978) pp. 2747-2753.
8. S. Subramanian, "Rapid Calculation of Defocused Partially Coherent Images," *Appl. Optics*, Vol. 20, No. 10, (May 15, 1981) pp. 1854-1857.
9. M. M. O'Toole and A. R. Neureuther, "Influence of Partial Coherence on Projection Printing," *Dev. Semicond. Microlithography IV*, SPIE Vol. 174, (1979) pp. 22-25.
10. S. Middlehoek, "Projection Masking, Thin Photoresist Layers and Interference Effects," *IBM Jour. Res. Devel.*, Vol. 14 (March, 1970) pp. 117-124.
11. J. E. Korka, "Standing Waves in Photoresists," *Appl. Optics*, Vol. 9, No. 4 (April, 1970) pp. 969-970.
12. D. F. Ilten and K. V. Patel, "Standing Wave Effects in Photoresist Exposure," *Image Technol.*, (Feb/March, 1971) pp. 9-14.
13. D. W. Widmann, "Quantitative Evaluation of Photoresist Patterns in the 1µm Range," *Appl. Optics*, Vol. 14, No. 4 (April, 1975) pp. 931-934.
14. F. H. Dill, "Optical Lithography," *Trans. Electron Dev.*, Vol. ED-22, No. 7 (July, 1975) pp. 440-444.
15. F. H. Dill, et al, "Characterization of Positive Photoresist," *Trans. Electron Dev.*, Vol. ED-22, No. 7, (July, 1975) pp. 445-452.
16. M. Born and E. Wolf, *Principles of Optics*, Pergamon Press (Oxford: 1965) pp. 556-592.
17. B. J. Lin, "Deep-UV Conformable Contact Photolithography for Bubble Circuits," *IBM Jour. Res. Devel.*, Vol. 20 (May, 1976) pp. 213-221.
18. W. G. Heitman and P. M. van den Berg, "Diffraction of Electromagnetic Waves by a Semi-Infinite Screen in a Layered Medium," *Canadian Jour. Phys.*, Vol. 53, No. 14, (July 15, 1975) pp. 1305-1317.
19. B. J. Lin, "Electromagnetic Near-Field Diffraction of a Medium Slit," *Jour. Optical Soc. Amer.*, Vol. 62, No. 8 (Aug., 1972) pp. 976-981.
20. D. J. Kim, W. G. Oldham and A. R. Neureuther, "Development of Positive Photoresist," *Trans. Electron. Dev.*, Vol. ED-31, No. 12, (Dec, 1984) pp. 1730-1736.